

Fluctuation-driven magnetic fields in the Madison Dynamo Experiment

E. J. Spence, M. D. Nornberg, R. A. Bayliss, R. D. Kendrick, and C. B. Forest

Citation: *Phys. Plasmas* **15**, 055910 (2008); doi: 10.1063/1.2890753

View online: <http://dx.doi.org/10.1063/1.2890753>

View Table of Contents: <http://pop.aip.org/resource/1/PHPAEN/v15/i5>

Published by the [American Institute of Physics](#).

Related Articles

A study of thermal counterflow using particle tracking velocimetry

[Phys. Fluids](#) **23**, 107102 (2011)

On electric fields created by quantized vortices
[Low Temp. Phys.](#) **37**, 884 (2011)

Torsional oscillation of vortex tangles. Possible applications to oscillations of solid 4He
[Low Temp. Phys.](#) **37**, 408 (2011)

Eddy damped quasinormal Markovian simulations of superfluid turbulence in helium II
[Phys. Fluids](#) **22**, 125103 (2010)

Comments on the article "Electric properties of metallic nanowires obtained in quantum vortices of superfluid helium," by

E. B. Gordon, A. V. Karabulin, V. I. Matyushenko, V. D. Sizov, and I. I. Khodos, *Fiz. Nizk. Temp.* **36**, 740 (2010)

[
[Low Temp. Phys.](#) **36**, 590 (2010)

]
[Low Temp. Phys.](#) **36**, 1107 (2010)

Additional information on *Phys. Plasmas*

Journal Homepage: <http://pop.aip.org/>

Journal Information: http://pop.aip.org/about/about_the_journal

Top downloads: http://pop.aip.org/features/most_downloaded

Information for Authors: <http://pop.aip.org/authors>

ADVERTISEMENT



HAVE YOU HEARD?

Employers hiring scientists
and engineers trust
physicstodayJOBS



<http://careers.physicstoday.org/post.cfm>

Fluctuation-driven magnetic fields in the Madison Dynamo Experiment^{a)}

E. J. Spence,^{1,b)} M. D. Nornberg,² R. A. Bayliss,³ R. D. Kendrick,⁴ and C. B. Forest^{4,c)}

¹*Eidgenössische Technische Hochschule Zürich, Institut für Geophysik,
Schafmattstrasse 30, CH-8093 Zürich, Switzerland*

²*Princeton Plasma Physics Laboratory, Princeton University, Princeton, New Jersey 08544, USA*

³*Department of Engineering Physics, University of Wisconsin-Madison, 1500 Engineering Drive,
Madison, Wisconsin 53706, USA*

⁴*Department of Physics, University of Wisconsin-Madison, 1150 University Avenue, Madison,
Wisconsin 53706, USA*

(Received 18 November 2007; accepted 13 February 2008; published online 10 April 2008)

Turbulent fluctuations in the velocity and magnetic fields of electrically conducting fluids have been experimentally shown to be capable of inducing large-scale magnetic fields. Here, simulations of the Madison Dynamo Experiment are used to qualitatively reproduce these experimental results. Due to the high magnetic Prandtl number of the simulations, $Pm=0.08$ vs $Pm \sim 10^{-5}$ for liquid sodium, the simulations do not identically reproduce the fluctuation levels of the experiment's magnetic and velocity fields. Nonetheless, the simulations reproduce the qualitative behavior of the fluctuation-induced large-scale magnetic field as a function of applied field magnitude and magnetic Reynolds number. The scaling of the induced dipole moment as a function of Reynolds number is also presented, demonstrating that the nature of the fluctuations in the simulations changes after a critical value of the Reynolds number is crossed, resulting in a change in the direction of the induced dipole moment. Experimental conditions using corotating impellers are presented, demonstrating that the induced dipole moment may be dependent on the shear layer present in the counter-rotating case. Measurements of velocity field fluctuations are examined to determine the possibility of an inhomogeneous turbulent resistivity. © 2008 American Institute of Physics.
[DOI: 10.1063/1.2890753]

I. INTRODUCTION

If the velocity and magnetic fields of a magnetohydrodynamic (MHD) system are expanded into their mean and fluctuating components, $\mathbf{B}=\langle\mathbf{B}\rangle+\tilde{\mathbf{B}}$ and $\mathbf{V}=\langle\mathbf{V}\rangle+\tilde{\mathbf{V}}$, then the mean magnetic induction equation takes the form

$$\frac{\partial\langle\mathbf{B}\rangle}{\partial t}=Rm\nabla\times(\langle\mathbf{V}\rangle\times\langle\mathbf{B}\rangle+\langle\tilde{\mathbf{V}}\times\tilde{\mathbf{B}}\rangle)+\nabla^2\langle\mathbf{B}\rangle, \quad (1)$$

where $Rm=\mu_0\sigma av_0$ is the magnetic Reynolds number, σ is the fluid's electrical conductivity, a is a length scale, and v_0 is a characteristic speed. The new term in the equation, $\mathcal{E}=\langle\tilde{\mathbf{V}}\times\tilde{\mathbf{B}}\rangle$, known as the turbulent electromotive force (EMF), results from the coherent interaction of velocity and magnetic field fluctuations. The fact that fluctuations can generate currents has been known for many years.¹⁻⁴ Such fluctuation-driven currents are sometimes examined in the paradigm of mean-field electrodynamics,^{5,6} whereby the currents are expanded in terms of the mean magnetic field.

Despite the many decades since the theoretical discovery of fluctuation-driven currents, their experimental examination has been relatively lacking. Steenbeck and collaborators⁷ examined the flow of liquid sodium through a folding channel, and detected an electromotive force, but their flow was well prescribed. Pétrélis *et al.* have postulated⁸ that fluctuations may be responsible for discrep-

ancies between a laminar model and the magnetic field measurements in their sodium experiment. The results of Spence *et al.* show that fluctuations can lead to a time-averaged magnetic field that opposes the experiment's dominant magnetic field.^{9,10} The nature of the fluctuations that generate these currents, however, remains an area of study.

Here we qualitatively reproduce the experimental results of the Madison Dynamo Experiment using numerical simulations. In Sec. II, we show that the relatively high value of viscosity used in the simulations results in magnetic and velocity fields that fail to reproduce the fluctuation levels measured in the experiment. Nonetheless, in Sec. III it is shown that these simulations qualitatively reproduce the scaling of the experimentally measured induced dipole moment, a magnetic field component that cannot be generated by the mean axisymmetric velocity field. In Sec. IV, we present the measured fluctuation-driven currents for the case of corotating impellers. This is followed, in Sec. V, by an examination of the possible role the β effect may play in the generation of these magnetic fields.

II. FLUCTUATION LEVELS

The Madison Dynamo Experiment is a one-meter-diameter sphere of flowing liquid sodium. A velocity field is generated in the experiment by a pair of impellers attached to shafts that enter the sphere through each pole.¹¹ The impellers rotate in counter- or corotating directions and generate an axisymmetric mean velocity field. With a fluid Reynolds number of $Re \sim 10^7$, the flowing sodium is very turbulent.

^{a)}Paper N12 2, Bull. Am. Phys. Soc. 52, 189 (2007).

^{b)}Invited speaker.

^{c)}Electronic mail: cbforest@wisc.edu.

Experiments consist of applying an approximately dipolar external magnetic field to the flowing sodium, and measuring the induced magnetic field internal and external to the sphere using Hall-effect sensors. Since the maximum speed of the impellers is known, and occurs at the tip of the impeller, Rm_{tip} , the magnetic Reynolds number based on the impeller tip speed, is used as the magnetic Reynolds number of the experiment.

Three-dimensional direct numerical simulations of the experiment are also performed. The simulation solves the momentum and magnetic induction equations in a spherical harmonic basis truncated at a spherical harmonic degree that is sufficiently high to resolve all relevant scales; details of the simulation code have been given previously.¹² The simulation contains two forcing regions that represent the experiment's impellers, and contains an externally applied dipolar magnetic field. The ability of the simulations to replicate experimental results is limited by the level of turbulence that can be computed in a reasonable amount of time. This is set by the magnetic Prandtl number, $Pm = Rm/Re = \nu/\eta$, the ratio of the fluid viscosity to electrical resistivity. All simulations presented in this paper have been computed with $Pm = 0.08$ (compared to $Pm \sim 10^{-5}$ for liquid sodium), except as noted in Sec. III.

The velocity field of the experiment is measured in an identical-scale water model using laser Doppler velocimetry (LDV).^{13,11} The θ and ϕ components of the velocity field, measured near the equator ($r = 38$ cm, $\theta = 1.5$), for the impellers counter-rotating at a rate of 800 revolutions per minute (RPM) ($Rm_{\text{tip}} \approx 80$, assuming the conductivity of sodium), are given in Figs. 1(a) and 1(b). Fluctuations over 100% of the mean are typical. The fluctuation levels of the two components are approximately the same, indicating isotropic fluctuations, a feature common throughout the sphere. To compare the effectiveness of simulations at reproducing the fluctuation levels of the experiment, the same components of the velocity field, calculated at the same position, from a simulation with $Rm = 80$, are presented in Figs. 1(c) and 1(d). The fluctuation level of the simulation is quite a bit smaller than the data for the θ component, while the ϕ component has much larger fluctuations than the data. Clearly the fluctuations in the simulation are not isotropic, though it is not currently known why this is the case. Though the boundary layers in the simulation are thicker than in the experiment, due to the simulation's higher viscosity, the measurement point is still far from the edge and should not be affected by the boundary.

A similar comparison can be done with the magnetic field. The θ and ϕ components of the magnetic field, measured at two positions within the sphere near the equator ($r = 38$ cm, $\theta = 1.5$, and $\theta = 1.0$ for the θ and ϕ components, respectively), for the impellers counter-rotating at a rate of 800 RPM, are given in Figs. 2(a) and 2(b). The fluctuation levels of the two components are not the same, due to the fact that the two fields are not being measured at the same location because of diagnostic limitations. Simulations of this field, with $Rm = 80$, are presented in Figs. 2(c) and 2(d). The fluctuation levels of the simulation are significantly larger than the measured data. This may be explained by the

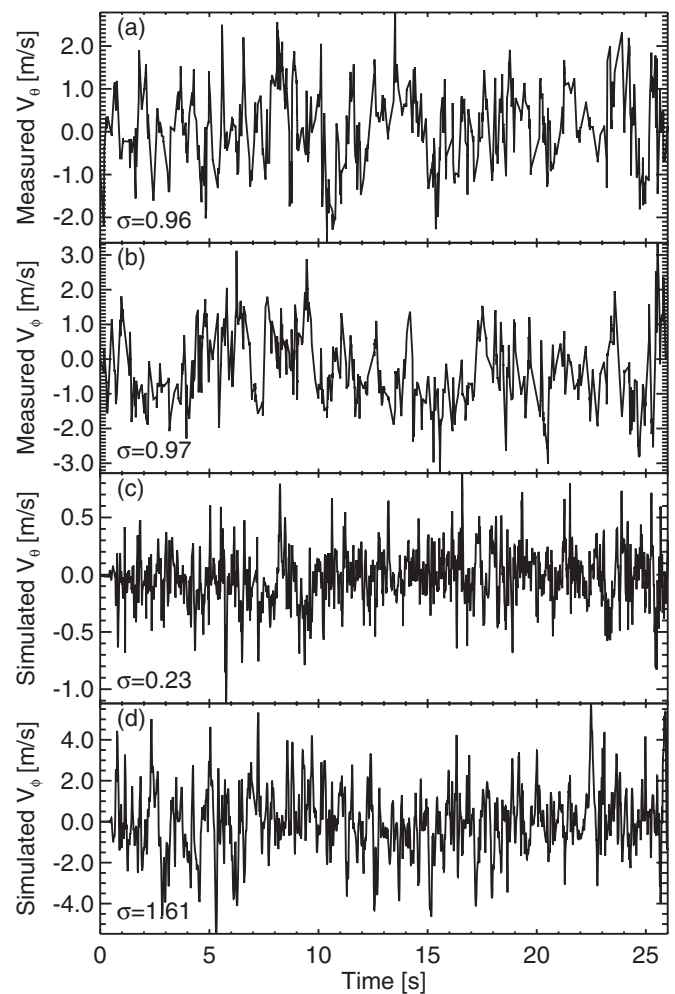


FIG. 1. Velocity field components of the Madison Dynamo Experiment, vs time, at $r = 38$ cm and $\theta = 1.5$. [(a) and (b)] θ and ϕ components of the velocity field as measured in an identical-scale water model of the experiment, for the impellers counter-rotating at 800 RPM. [(c) and (d)] Simulations of the θ and ϕ components of the velocity field, with $Rm = 80$. The standard deviation of the fluctuations is given in the lower left corner of each panel.

large magnetic Prandtl number of the simulation, which results in a much smaller resistive diffusion scale than in the experiment. This causes the magnetic field to be amplified to large values at much smaller scales, resulting in larger magnetic field fluctuations. Like the simulated fluctuation levels of the velocity field components, the simulated fluctuation levels of the magnetic field components at the same locations are not the same, though these data are not presented in Fig. 2. Thus, the simulated magnetic field fluctuations are not isotropic.

The fluctuation levels of the velocity and magnetic fields found in the simulations do not match those measured in the experiment. This is most likely due to the large magnetic Prandtl number of the simulations, though differences in the details of the forcing used to push the fluid may also play a role. Nonetheless the fluctuations are still large and the flow is very turbulent. As will be shown below, the simulations agree qualitatively with experimental measurements of the

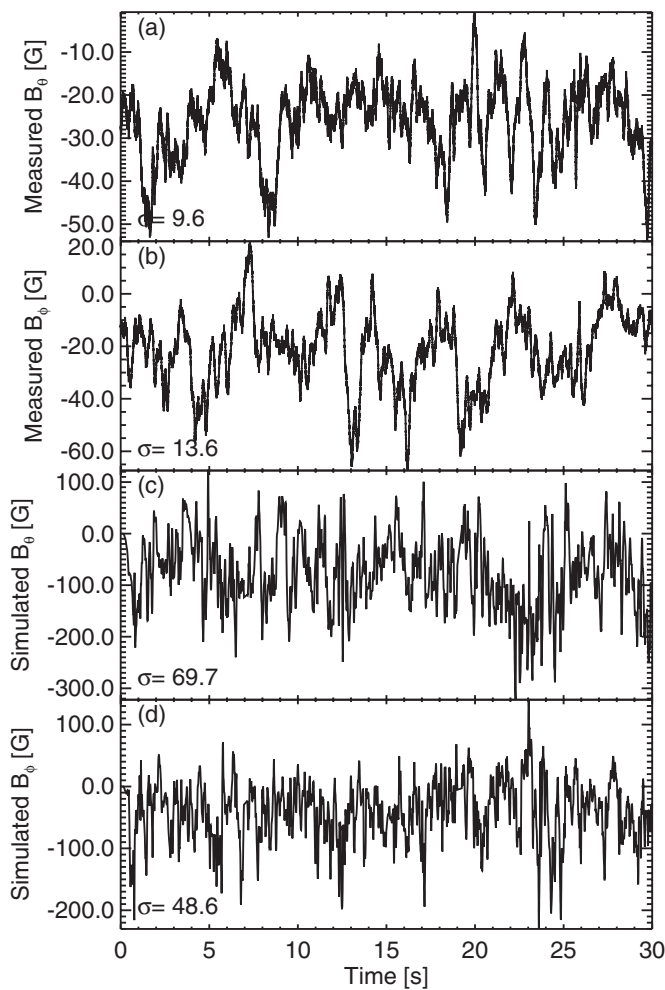


FIG. 2. Magnetic field components of the Madison Dynamo Experiment, vs time, at $r=38$ cm and $\theta=1.5$ and 1.0 for the θ and ϕ components, respectively. [(a) and (b)] θ and ϕ components of the magnetic field as measured within the sodium, for the impellers counter-rotating at 800 RPM and an applied field of 60 G. [(c) and (d)] Simulations of the θ and ϕ components of the magnetic field, with $Rm=80$. The standard deviation of the fluctuations is given in the lower left corner of each panel.

external induced dipole moment, and as such are helpful for developing intuition about the physical processes at work in the experiment.

III. SCALING OF THE INDUCED DIPOLE MOMENT

It has been shown that simply connected volumes with axisymmetric flows are incapable of inducing external dipole moments when exposed to an external magnetic field.⁹ Since the mean axisymmetric velocity field is incapable of inducing dipole moments, fluctuations in the velocity and magnetic fields, the $\langle \tilde{\mathbf{V}} \times \tilde{\mathbf{B}} \rangle$ term in Eq. (1), must be responsible. Though the fluctuation levels of the simulations are not the same magnitude as those measured in the experiment, we believe that much of the physics of the experiment is being captured by the simulations, at least qualitatively. For example, Fig. 3 presents the time-averaged induced dipole moment measured on the surface of the sphere versus magnitude of the externally applied field, with the impellers counter-rotating at 1000 RPM ($Rm_{tip}=100$). Also plotted in

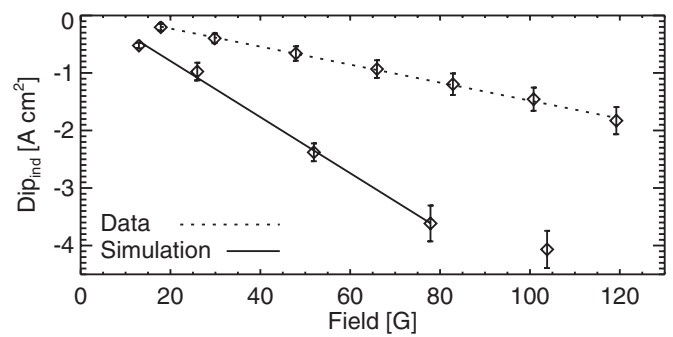


FIG. 3. Induced dipole moment vs magnitude of applied field, for impellers counter-rotating at 1000 RPM, for data measured on the Madison Dynamo Experiment and simulations performed with $Rm=100$. The error bars are one standard deviation of the fluctuations of the dipole moment. Negative values of dipole moment indicate opposition to the applied field. Saturation of the induced dipole moment is observed in the simulation data.

this figure is the averaged induced dipole moment as calculated by simulation, for $Rm=100$. As might be expected when the Lorentz force is not the dominant force in the system (the applied field is weak), the dipole moment induced by the experiment scales linearly with applied field. The dipole induced in the simulation is also linear in applied field for the range of applied field where the Lorentz force is weak (applied field magnitude less than 80 G). As the field is increased, however, the magnitude of the induced dipole begins to drop relative to the expected linear trend, indicating saturation of the effect. Since inertia is less important in the simulation than in the experiment, due to the much higher value of viscosity, the saturation of the induced dipole moment occurs at a much lower field magnitude than in the experiment. Saturation of the induced dipole moment in the experiment has not yet been observed.

We can also plot the magnitude of the dipole moment versus Rm for both the experimental measurements and simulations. These are presented in Fig. 4. The measured dipole moment is quadratic in magnetic Reynolds number, until about $Rm_{tip}=60$, after which the trend is somewhat linear. A similar trend is found in the simulation results, though for a smaller range of Rm . As with Fig. 3, the magnitude of the induced dipole moment is significantly larger in the simulations than the measured data.

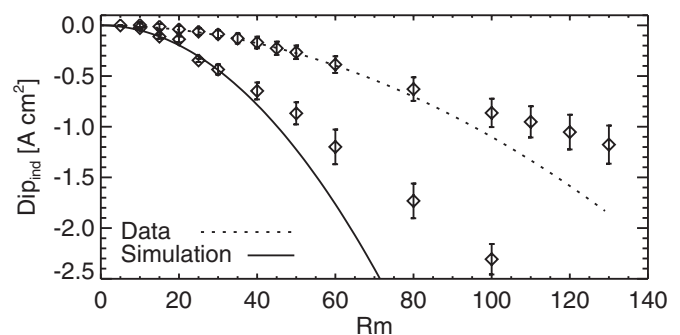


FIG. 4. Induced dipole moment vs Rm , for an applied field of 50 G, for data measured on the Madison Dynamo Experiment and data calculated using simulations. At low Rm , the dependence is quadratic.

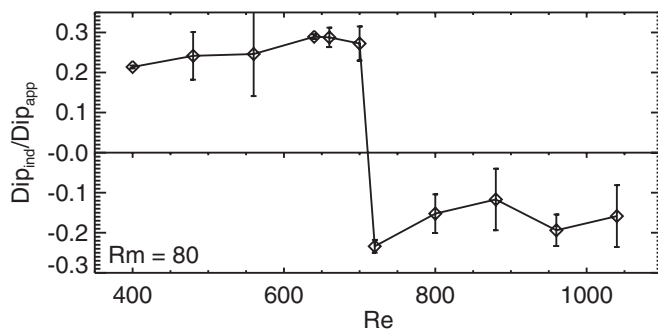


FIG. 5. Induced dipole moment scaled to the applied dipole moment vs Re , for simulations of the Madison Dynamo Experiment performed with $Rm = 80$. Positive values indicate a reinforcing of the applied field, and negative values indicate opposition.

It should be noted that the simulation results presented in Fig. 4 are not calculated at constant Pm , since at low values of magnetic Reynolds number $Pm = 0.08$ does not lead to turbulent flows, and thus produces no dipole moment. For the data points below $Rm = 60$, a constant value of $Re = 800$ is used to make sure that the resulting flows are turbulent. All other values in the figure use $Pm = 0.08$.

To examine the dependence of the induced dipole moment on viscosity, simulations are performed at a constant $Rm = 80$, but with varying Re . The result of this series of simulations is presented in Fig. 5. At low magnetic Prandtl number (high Re , the regime of the experiment), the induced dipole moment opposes the dipole moment due to the externally applied magnetic field, the result measured in the experiment. As the Reynolds number is lowered, however, the orientation of the induced dipole moment suddenly changes

sign and reinforces the applied field. The cause of this change is still under investigation, but appears to be related to a change in the nature of the velocity field fluctuations.

IV. FLUCTUATION-DRIVEN MAGNETIC FIELDS

If an external magnetic field is applied to the flowing sodium, and the mean axisymmetric velocity and magnetic fields are known, then the contributions to the induced field due to the mean velocity field, $\langle \mathbf{V} \rangle \times \langle \mathbf{B} \rangle$, and the fluctuation-driven field, $\langle \tilde{\mathbf{V}} \times \tilde{\mathbf{B}} \rangle$, can be calculated, assuming that the current density is divergence-free. Such analyses have been previously reported for counter-rotating flows using experimental measurements¹⁰ and simulations¹² of the Madison Dynamo Experiment. These studies found that the fluctuation-driven currents generated an external dipole moment, as discussed in Sec. III, and induced a fluctuation-driven magnetic field that opposed the experiment's dominant magnetic fields. In the poloidal direction, the fluctuation-driven field opposed the externally applied field. In the toroidal direction, it opposed the field due to the mean velocity field advecting the applied field (the field due to the ω effect). The strength of the fluctuation-driven fields was found to be much stronger in the experiment than in the simulation.

To further explore the physics of fluctuation-driven currents, the same analysis has been performed on Madison Dynamo Experiment measurements for the case of the impellers corotating (rotating in the same direction) at 800 RPM. To perform this analysis, the mean axisymmetric velocity and magnetic fields are needed. These have been measured, as described previously,^{9-11,13} and are presented with their corresponding fits in Figs. 6 and 7. As one might ex-

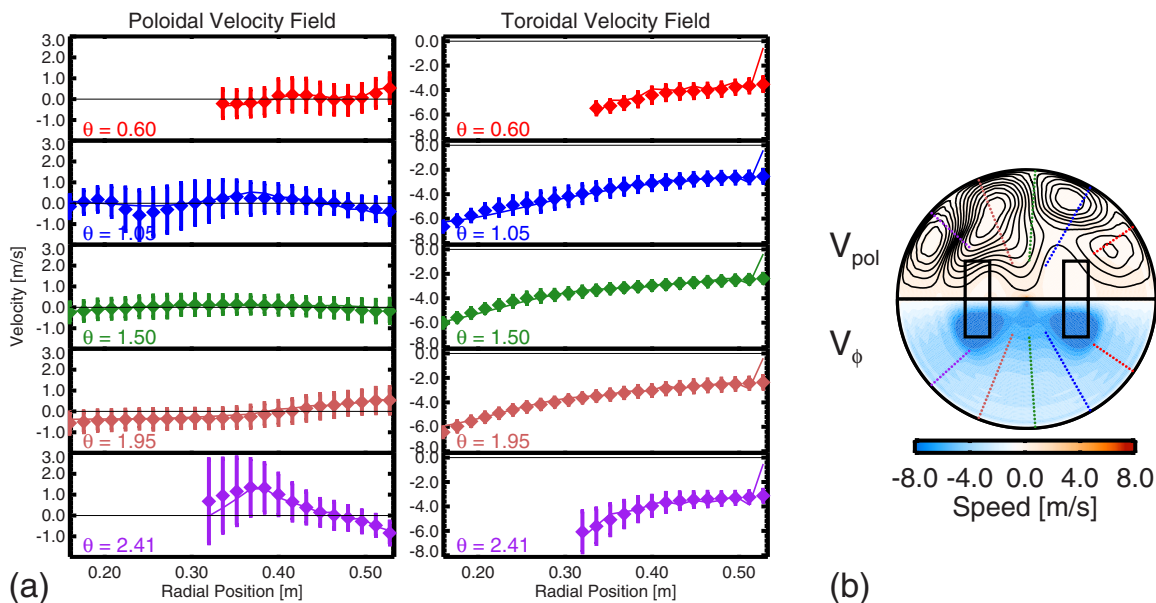


FIG. 6. (Color online) Velocity fields measured in the water model of the Madison Dynamo Experiment. (a) Mean measured velocity field as a function of radial position, for impellers corotating at 800 RPM. The fit (solid lines) represents values predicted by a spherical harmonic expansion fit to the data (diamonds). Error bars represent the root-mean-square fluctuation levels of the signals. (b) The reconstructed velocity field, with the axis of symmetry oriented horizontally. Streamlines of the poloidal field are in the upper hemisphere and the toroidal field strength is in the lower hemisphere. Measurement positions are indicated with dots, and the impeller positions are indicated with rectangles.

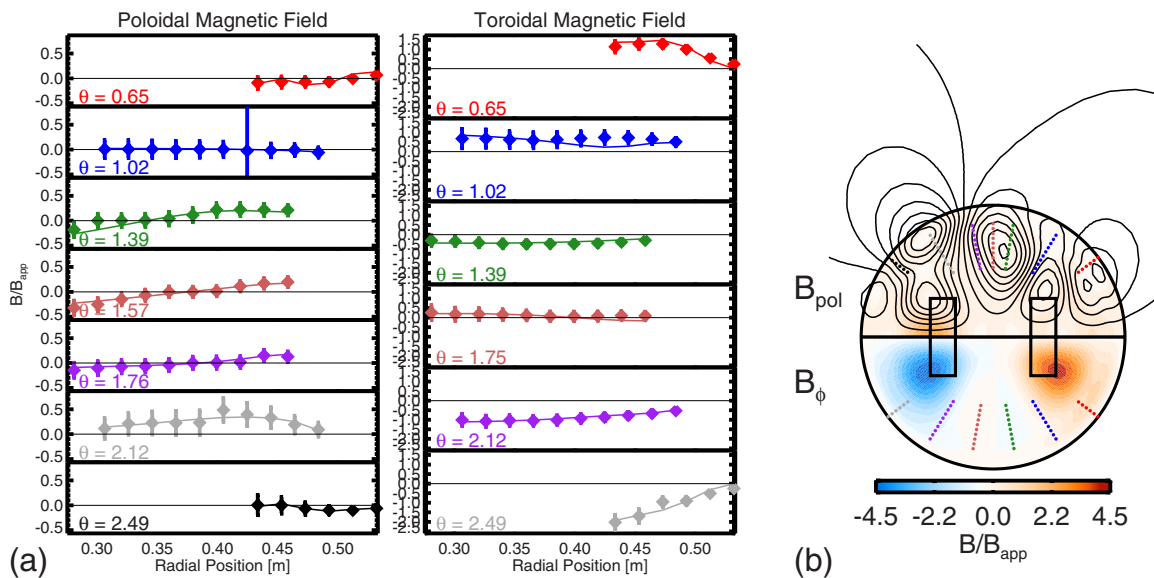


FIG. 7. (Color online) Induced magnetic fields measured in the Madison Dynamo Experiment. (a) Mean measured poloidal and toroidal field values, scaled to the magnitude of the applied field (50 G), for impellers corotating at 800 RPM. (b) The reconstructed field. In both panels, the conventions are as in Fig. 6.

pect, since the two impellers rotate in the same direction, there is a strong toroidal velocity field. The poloidal component is more complex, dominated by a four-cell structure. The poloidal field is not symmetric about the equator, due to the preferred direction of the poloidal forcing. Interestingly, the measured magnetic field does not contain an induced dipole moment, in contrast to the counter-rotating case.

Using the measurements of the mean velocity and magnetic fields, one can separate the magnetic field induced by the mean velocity field interacting with the mean magnetic field, $\langle \mathbf{V} \times \langle \mathbf{B} \rangle$, and the field induced by fluctuations, $\langle \tilde{\mathbf{V}} \times \tilde{\mathbf{B}} \rangle$; these are presented in Fig. 8. Like the counter-rotating case, the magnetic field due to fluctuations makes a

significant contribution to the measured field, having a larger magnitude in many spots than the field due to the mean flow.

Clearly the lack of induced external dipole moment in this experimental configuration is indicative of a change in the nature of the fluctuations within the experiment as compared to the counter-rotating case. One distinguishing characteristic of the counter-rotating flow that is absent from the corotating flow is the presence of a toroidal shear layer at the equator. It is possible that eddies being formed at the shear layer are somehow associated with the fluctuation-driven currents that generate the induced dipole moment. Unfortunately, simulations have not yet been performed using this impeller configuration. This is an area of ongoing research.

V. INHOMOGENEOUS TURBULENT CONDUCTIVITY

One of the effects of turbulence on a conducting fluid is the effective enhancement of resistivity due to turbulence.⁵ Mean-field electrodynamics provides a method of addressing the turbulent EMF through a first-order smoothing approximation, whereby the EMF is expanded in terms of the mean magnetic field, $\mathcal{E}_i = \alpha_{ij} \langle \mathbf{B} \rangle_j + \beta_{ijk} \partial \langle \mathbf{B} \rangle_j / \partial x_k$. The term responsible for enhanced resistivity, assuming isotropic turbulence and no mean flow, is given by

$$\beta = \frac{1}{3} \int \langle \tilde{\mathbf{v}}(\mathbf{r}, t) \cdot \tilde{\mathbf{v}}(\mathbf{r}, t - \tau) \rangle d\tau. \quad (2)$$

For homogeneous turbulence, β is a scalar quantity that results in a turbulent EMF of the form $\mathcal{E} = -\beta \nabla \times \langle \mathbf{B} \rangle = -\beta \mu_0 \langle \mathbf{J} \rangle$. Hence, $\nabla \times \mathcal{E} = \beta \nabla^2 \langle \mathbf{B} \rangle$, from which it can be seen that the β term can be incorporated into an effective turbulent conductivity,

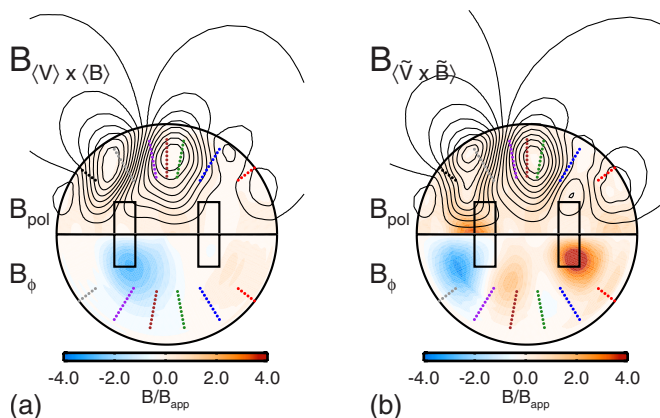


FIG. 8. (Color online) Two contributions to the measured induced magnetic field, calculated from measurements in the Madison Dynamo Experiment, for the impellers corotating at 800 RPM in the presence of an externally applied magnetic field. (a) Magnetic field due to the mean flow interacting with the mean magnetic field. (b) Magnetic field due to fluctuations. In both panels, the conventions are as in Fig. 6.

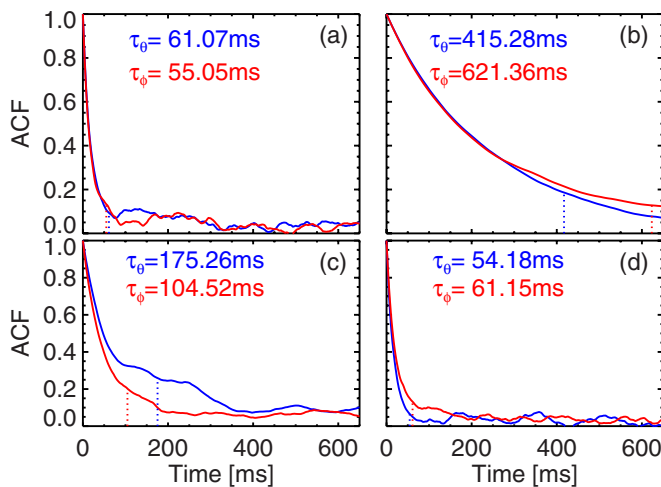


FIG. 9. (Color online) Autocorrelation functions of LDV velocity measurements for $Rm_{tip}=100$. The locations are (a) in the bulk flow above and behind the impeller ($r=45$ cm, $\theta=0.596$), (b) deep in the flow at the equator ($r=26$ cm, $\theta=1.50$), (c) near the wall ($r=53$ cm, $\theta=0.596$), and (d) near an impeller ($r=34$ cm, $\theta=0.596$). The correlation time is calculated for each velocity component using Eq. (5).

$$\sigma_T = \frac{\sigma}{(1 + \mu_0 \sigma \beta)}. \quad (3)$$

This relation is given in the high-conductivity limit, which assumes that the correlation time $\tau_{\text{corr}} \ll \mu\sigma\lambda_{\text{corr}}^2$, where λ_{corr} is the correlation length. As the correlation time becomes longer, the turbulent enhancement of the resistivity is reduced and so Eq. (3) may underestimate the effective conductivity. If the observed velocity fluctuations are due to eddies being convected past the measurement point, then correlation length scales with the mean flow scale length a so that $\tau_{\text{corr}} \ll \mu_0\sigma a^2$, the resistive diffusion time, which is 3 s for the experiment.¹¹

Overlooking the fact that the experiment has a mean flow, the β effect can be estimated from Eq. (2) with the measurements of the velocity field fluctuations and correlation times obtained from the water model of the experiment using LDV.¹¹ The turbulence in the experiment is isotropic, as demonstrated by Fig. 1, but not homogeneous, and thus β is not a constant. Under these conditions, the β -effect term is estimated to be

$$\beta(\mathbf{r}) = \frac{1}{3} \int_0^\infty \langle \tilde{\mathbf{v}}(\mathbf{r}, t) \cdot \tilde{\mathbf{v}}(\mathbf{r}, t - \tau) \rangle d\tau = \frac{1}{3} v_{\text{rms}}^2 \tau_{\text{corr}}, \quad (4)$$

where $\beta(\mathbf{r})$ is now a function over space, v_{rms} is the rms speed at the measurement point, τ_{corr} is the correlation time defined as

$$\tau_{\text{corr}} = |R_{ii}(0)|^{-1} \int_0^T |R_{ii}(\tau)| d\tau, \quad (5)$$

and $R_{ii}(\tau)$ is the autocorrelation function. Assuming axisymmetry, we have $\beta(\mathbf{r}) = \beta(r, \theta)$, which can be determined from the autocorrelation functions of the LDV measurements from Fig. 9. The turbulent conductivity σ_T can then be computed using Eq. (3); a contour plot value of σ_T/σ derived from the

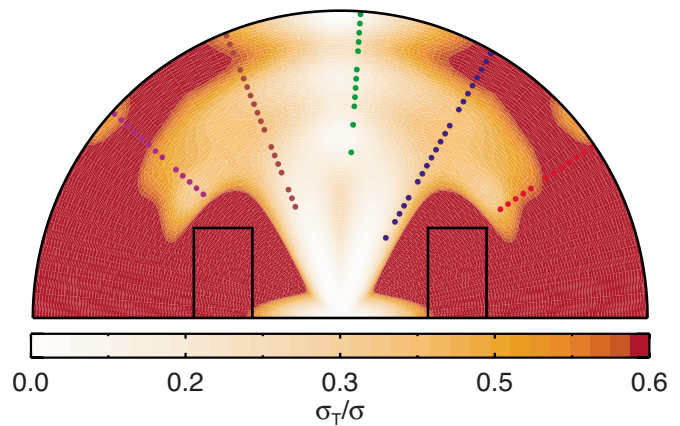


FIG. 10. (Color online) Contour plot of σ_T/σ created by a curve fit of v_{rms} and τ_{corr} measurements.

LDV measurements is shown in Fig. 10. Although σ_T is not uniform throughout the flow, on average the turbulence results in a 40% decrease in the effective conductivity of the fluid.

From Fig. 10, it is apparent that the effect is strongest in the shear layer at the equator. Though the velocity fluctuation levels at the equator are fairly weak compared with the rest of the flow, the correlation time is much longer as is evidenced in Fig. 9(b). Comparison with the correlation times in Fig. 9 shows that the criterion for the high-conductivity limit is satisfied throughout most of the flow but is perhaps only marginally satisfied near the shear layer at the equator where correlation times are much longer; the effective conductivity may not be as low as our estimate suggests. Nevertheless, this observation is consistent with the situation described by Colgate¹⁴ in which the shear layer develops a Kelvin–Helmholtz instability that governs the strength of the β effect. The effect also leads to strong gradients in the effective conductivity, which has been suggested as a possible mechanism for the turbulence-induced dipole moment.⁹

VI. DISCUSSION AND CONCLUSION

The fluctuation levels of the simulations, both velocity and magnetic, do not agree with the fluctuation levels measured in the experiment. The differences between the measurements and the simulations are twofold. First, the simulated fluctuation levels of the two components of the velocity field are not the same as one would expect for isotropic turbulence. This is similarly true for the simulated magnetic field, though these data are not presented here. The explanation for this discrepancy is not immediately clear. The positions being examined are far enough from the boundary layer and impeller-forcing region that edge and localized-forcing effects should not be important. Second, the magnitude of the simulated fluctuation levels do not agree with those experimentally measured. Further examination of these discrepancies will be a topic of future work.

The dipole moment that is induced by the simulations has a much larger magnitude than that which is measured in experiment. This may be related to the differences in the

fluctuations due to the differences in viscosity between the simulation and experiment. The high viscosity of the simulations would naturally result in fewer small eddies being formed, which might result in a higher turbulent conductivity in the simulation. However, previous work has noted that the magnetic field in the volume of the sphere due to turbulent fluctuations is greater in experiment than in simulations,^{10,12} so the hypothesis of a higher turbulent conductivity may not be true in general. Another possible explanation of the discrepancy is with regard to the value of Rm used in each system. The value of Rm used for the experiment, Rm_{tip} , is based on the impeller tip speed, and is likely significantly higher than the value of Rm one might find using the actual peak speed of the flow. If one were to drop the value of Rm used for the measurements in Fig. 4 by a factor of 2, then the simulation results would be in much better agreement with the data.

It should also be noted that the differences between simulation and experimental results may be affected by differences in the details of how the fluid is forced in the simulation versus the experimental impellers. While the resulting bulk flow is very similar to that experimentally measured, there are differences between that simulated and measured. Also the nature of the eddies that spill off the tips of the impellers may be very different from those that result from simulations of the same.

The lack of an external dipole moment in the case of corotating impellers suggests that the equatorial shear layer that is present in the counter-rotating-impeller case may be important for the induced external dipole moment. Future work on this topic will include simulating the corotating-impeller case, as well as using simulations to determine the nature of the fluctuations that are responsible for the induced dipole moment.

We have presented a rather simple analysis of the velocity field fluctuations which indicates that turbulent reduction of the conductivity is likely, though the estimate requires assuming that the experiment has no mean flow, which is of course incorrect. Unfortunately, no theory exists to estimate the level of turbulent conductivity in the presence of a mean flow. Nonetheless, a nonuniform conductivity is not the only

possible cause of the observed fluctuation-driven currents. Helical fluctuations, turbulent flux expulsion, and other effects cannot yet be ruled out. Exploration of the fluctuations in the experiment is a continuing line of research.

In summary, simulations of the Madison Dynamo Experiment do not generate fluctuation levels in the velocity and magnetic fields that agree with measurements. Nonetheless, simulations qualitatively reproduce the scalings of the induced dipole moment as measured in the Madison Dynamo Experiment. Measurements of the fluctuation-driven currents for the case of corotating impellers indicates that fluctuation-driven magnetic fields are a significant component of the total magnetic field, though no external dipole moment is induced. Examination of the fluctuation levels of velocity field in the water model of the experiment indicates that the turbulent modifications to the conductivity could be significant, though it is certainly not the only possible explanation for the measured and simulated fluctuation-driven magnetic fields.

¹M. Steenbeck and F. Krause, *Z. Naturforsch. A* **21**, 1285 (1966).

²F. Krause and M. Steenbeck, *Z. Naturforsch. A* **22**, 671 (1967).

³P. Odier, J.-F. Pinton, and S. Fauve, *Phys. Rev. E* **58**, 7397 (1998).

⁴M. Bourgoïn, L. Marié, F. Pétrélis, C. Gasquet, A. Guigon, J.-B. Luciani, M. Moulin, F. Namer, J. Burguete, A. Chiffaudel, F. Daviaud, S. Fauve, P. Odier, and J.-F. Pinton, *Phys. Fluids* **14**, 3046 (2002).

⁵K. Krause and K. H. Rädler, *Mean-field Magnetohydrodynamics and Dynamo Theory* (Pergamon, New York, 1980).

⁶H. K. Moffatt, *Magnetic Field Generation in Electrically Conducting Fluids* (Cambridge University Press, Cambridge, UK, 1978).

⁷M. Steenbeck, I. M. Kirko, A. Gailitis, A. P. Klyavinya, F. Krause, I. Y. Laumanis, and O. A. Lielausis, *Sov. Phys. Dokl.* **13**, 443 (1968).

⁸F. Pétrélis, M. Bourgoïn, L. Marié, J. Burguete, A. Chiffaudel, F. Daviaud, S. Fauve, P. Odier, and J.-F. Pinton, *Phys. Rev. Lett.* **90**, 174501 (2003).

⁹E. J. Spence, M. D. Nornberg, C. M. Jacobson, R. D. Kendrick, and C. B. Forest, *Phys. Rev. Lett.* **96**, 055002 (2006).

¹⁰E. J. Spence, M. D. Nornberg, C. M. Jacobson, C. A. Parada, N. Z. Taylor, R. D. Kendrick, and C. B. Forest, *Phys. Rev. Lett.* **98**, 164503 (2007).

¹¹M. D. Nornberg, E. J. Spence, R. D. Kendrick, C. M. Jacobson, and C. B. Forest, *Phys. Plasmas* **13**, 055901 (2006).

¹²R. A. Bayliss, C. B. Forest, M. D. Nornberg, E. J. Spence, and P. W. Terry, *Phys. Rev. E* **75**, 026303 (2007).

¹³C. B. Forest, R. A. Bayliss, R. D. Kendrick, M. D. Nornberg, R. O'Connell, and E. J. Spence, *Magnetohydrodynamics* **38**, 107 (2002).

¹⁴S. A. Colgate, *Astron. Nachr.* **327**, 456 (2006).